Journal of Engineering Mathematics **49:** 41–55, 2004.

The propagation and inhibition of an exothermic branched-chain flame with an endothermic reaction and radical scavenging

A. LAZAROVICI, S. KALLIADASIS[1], J.H. MERKIN, S.K. SCOTT[2] and P.L. SIMON[2]
Department of Applied Mathematics; [1]*Department of Chemical Engineering;* [2]*School of Chemistry, University of Leeds, Leeds, LS2 9JT, UK*

Received 18 February 2003; accepted in revised form 21 July 2003

Abstract. The effects of the endothermic decomposition of an inhibitory species W to form a radical scavenger on a laminar, pre-mixed flame supported by an exothermic second-order branching reaction are considered. This work extends a previous study, where the effects of the radical scavenger S were ignored. Two cases are identified, dependent on a parameter β measuring the relative rate of the decomposition of W. These are described by an high-activation-energy asymptotic analysis and through numerical integration of the propagating-flame equations for representative parameter values. For larger values of β the effect of the radical scavenger is to introduce a critical value of the heat-loss parameter α for flame propagation. For smaller values of β, where there is a critical value of α without any S being produced, the effect is to lower this critical value. In both cases the effect of the radical scavenger is to reduce the propagation speed and, if sufficient amounts of S are produced from the decomposition of W, to totally suppress flame propagation, even without any heat loss.

Key words: combustion, endothermic inhibition, high-activation-energy asymptotics, propagating flames, radical scavenger

1. Introduction

In a previous paper [1] we described a model for the propagation of a flame driven by an exothermic reaction subject to endothermic chemical processes. These consisted of the endothermic decomposition of an inhibitor species leading to the formation of a 'radical scavenger'. This, in turn, acted as a catalyst for the removal of active radicals through an additional termination step. It was shown in [1] that these endothermic processes could have significant effects on flame propagation, producing considerable reductions in the flame speed and giving the possibility of flame inhibition.

It is the purpose of this paper to examine this model in more detail. A simplified version of the model, in which the decomposition of the inhibitor was the only endothermic process, was considered in [2]. There the model consisted of a second-order, exothermic reaction for the fuel and a first-order reaction for the inhibitor. In [2] it was seen that the high-activation-energy limit provided clear insights into the nature of flame propagation or inhibition, as well as giving a basic understanding of the structure of the flame. An alternative version of this problem in which the reaction for the fuel was a first-order process has been considered in [3], where again the high-activation-energy asymptotics provided a useful guide into the nature of the flame propagation. A prototype version of the model considered in [2], where the Arrhenius temperature dependence of the kinetics is replaced by a step-function behaviour, [4], has also revealed that the endothermic decomposition of the inhibitor can have significant effects on flame propagation. It is high-activation-energy asymptotics that we mostly concentrate on

here, paying particular attention to the effect that the radical scavenger can have on flame inhibition.

Our main aim here, through the analysis of a simple model, is to assess the contributions made to flame inhibition by heat loss through some endothermic process – thermal effects, and by the removal of the active radical – chemical effects. Both thermal and chemical effects have been observed experimentally to have a strong influence on flame inhibition and quenching of both premixed [5, 6] and counter-flow flames [7–9]. One motivation for the form of the heat-loss term in our model is the vaporization of a water mist. This effect has a strong temperature dependence, perhaps through some activation energy, and will depend on the local concentrations of the water mist (as in our model). However, this is clearly a gross simplification of the physics of this phase-transition but our model may be useful, giving some qualitative comparison with experimental data, or at least indicate the main mechanisms involved in flame inhibition by this process. In this scenario, the chemical effects can be thought of as arising from salts dissolved within the water mist. These have also been observed to have strong quenching effects on flame propagation and our model may give some insights into how these two processes, thermal and chemical effects, compete to inhibit flame propagation.

We start by describing our model and setting up the corresponding equations for the propagating flame.

2. Model

Our kinetic scheme is based on the Zel'dovich-Liñan model, see [10–12] for example, in which a reactant A and a radical intermediate X combine to form a set of inert products P through the following sequence of initiation, branching and termination steps

$$A \to X \qquad \text{rate } = k_i(T)\, a, \tag{1}$$

$$A + X \to 2X \qquad \text{rate } = k_b(T)\, a\, \overline{x}, \tag{2}$$

$$X + X \to P \qquad \text{rate } = k_t\, \overline{x}^2, \quad q_t > 0, \tag{3}$$

where a and $\overline{x}$ are the concentrations of species A and X respectively and T is (absolute) temperature. The rate coefficients of the initiation and branching steps (1) and (2) have an Arrhenius temperature dependence of the form

$$k_i(T) = k_{i,0}\, \exp(-E_i/RT), \qquad k_b(T) = k_{b,0}\, \exp(-E_b/RT).$$

Here E_i and E_b are the respective activation energies, R is the universal gas constant and $k_{i,0}$ and $k_{b,0}$ are constants (pre-exponential factors). The termination step (3) is assumed to be independent of temperature and to be an exothermic process with exothermicity q_t.

Our extension to this basic scheme is the inclusion of a quenching effect through the additional steps

$$W \to r\,S \qquad \text{rate } = k_w(T)\, \overline{w}, \quad q_w < 0, \tag{4}$$

$$S + X \to S + Q \qquad \text{rate } = k_s\, \overline{x}\, s, \tag{5}$$

where $\overline{w}$ and s are the concentrations of species W and S, respectively. Step (4) represents the endothermic decomposition of an inhibitor species W to form the radical scavenger S

(for $r > 0$) and is taken to have an Arrhenius temperature dependence with activation energy E_w, *i.e.*, $k_w(T) = k_{w,0} \exp(-E_w/RT)$. The radical scavenger acts catalytically to remove the radical X via step (5), which is assumed to be temperature independent and to have zero exothermicity.

We can expect step (1) to be a relatively slow process in the flame context that will be neglected in our model. Its role is just to seed some radical X locally into the the system to enable the reaction to proceed. We make the usual assumption of constant pressure for slow-speed laminar flames and take the physical parameters to be independent of temperature. This leads to the following set of equations, written in terms of a travelling co-ordinate $\overline{y}$ moving with the flame,

$$\kappa T'' + \overline{c}\,\sigma C_p T' + q_t k_t \overline{x}^2 + q_w k_w(T)\overline{w} = 0, \quad D_A a'' + \overline{c}\,a' - k_b(T) a\,\overline{x} = 0, \tag{6}$$

$$D_W \overline{w}'' + \overline{c}\,\overline{w}' - k_w(T)\overline{w} = 0, \quad D_X \overline{x}'' + \overline{c}\,\overline{x}' + k_b(T) a\,\overline{x} - 2k_t\overline{x}^2 - k_s \overline{x} s = 0,$$

where primes denote differentiation with respect to $\overline{y}$. The concentrations of the chemical inhibitor W and radical scavenger S, which is created directly from the decomposition of W, are related by the conservation law

$$s = r(w_0 - \overline{w}) \tag{7}$$

In the above D_A, D_W and D_X are the diffusion coefficients for species A, W and X, respectively, κ is the thermal conductivity, C_p and σ are the specific heat at constant pressure and the density (both assumed constant); $\overline{c}$ is the (constant) speed of propagation of the flame. We assume that $\overline{c} > 0$. Ahead of the flame the system is in its unreacted state with

$$a = a_0,\ \overline{w} = w_0,\ T = T_a,\ \overline{x} = 0,\ s = 0, \tag{8}$$

where a_0 and w_0 are the (constant) concentrations of the fuel A and inhibitor W and T_a is the ambient temperature.

Having $T_a \neq 0$ ahead of the flame causes a problem, the so-called 'cold boundary problem', since, in the present context, reaction rate (4) is non-zero. Several approaches have been suggested to remove this difficulty. One is to set $T_a = 0$. This is not a particularly unrealistic thing to do as the temperatures that can be achieved within a flame are generally very much higher than typical ambient temperatures and, at these ambient temperatures, the Arrhenius functions give values that are usually very small. This is the approach we adopt here. An alternative approach is to invoke an 'ignition temperature' T_i (say), $T_i > T_a$, taking the temperature dependence, here $k_b(T)$ and $k_w(T)$, to be zero for temperatures $T < T_i$. This approach has a drawback in that it introduces the additional and somewhat artificial parameter T_i. The results obtained from these two approaches have been shown to agree in the limit as $T_i \to 0$ [13].

We wish to exploit high-activation-energy asymptotics. This leads us to introduce the dimensionless variables, following an initial development of this idea in [14] and used in [2, 3],

$$T = T_{\text{ref}}\, u, \quad a = a_0(1 - v), \quad \overline{w} = w_0(1 - w), \quad \overline{x} = x\left(\frac{k_{b,0} a_0 \mathrm{e}^{-1/2\epsilon}}{2k_t}\right), \tag{9}$$

where (with $T_a = 0$) the reference temperature T_{ref} is defined as $T_{\text{ref}} = \dfrac{q_t a_0}{2\sigma C_p}$ and $\epsilon = \frac{RT_{\text{ref}}}{2E_b}$ is our activation energy parameter. If we apply (9) in Equations (6, 7) we obtain the dimensionless equations for our model as

$$u'' + c\,u' + x^2 - \alpha(1-w)\,\exp\left(-\frac{\mu(1-u)}{\epsilon u}\right) = 0, \tag{10}$$

$$\frac{1}{L_A}v'' + c\,v' + (1-v)\,x\,\exp\left(-\frac{(1-u)}{2\epsilon u}\right) = 0, \tag{11}$$

$$\frac{1}{L_W}w'' + c\,w' + \beta(1-w)\,\exp\left(-\frac{\mu(1-u)}{\epsilon u}\right) = 0, \tag{12}$$

$$\delta\left(\frac{1}{L_X}x'' + c\,x'\right) + x\,(1-v)\,\exp\left(-\frac{(1-u)}{2\epsilon u}\right) - x^2 - \rho x\,w = 0. \tag{13}$$

The dimensionless travelling co-ordinate y and flame speed c are given by

$$y = \overline{y}\left(\frac{\sigma C_p a_0 k_{b,0}^2}{2\kappa k_t \mathrm{e}^{1/\epsilon}}\right)^{1/2}, \quad c = \overline{c}\left(\frac{2\sigma C_p k_t \mathrm{e}^{1/\epsilon}}{\kappa a_0 k_{b,0}^2}\right)^{1/2}. \tag{14}$$

Here L_A, L_W and L_X are the Lewis numbers associated with species A, W and, X, respectively, *viz.*

$$L_A = \frac{\kappa}{\sigma C_p D_A}, \quad L_W = \frac{\kappa}{\sigma C_p D_W}, \quad L_X = \frac{\kappa}{\sigma C_p D_X}$$

The other dimensionless (kinetic) parameters are given by

$$\alpha = \frac{4(-q_w)k_{w,0}k_t w_0 \mathrm{e}^{(1-\mu)/\epsilon}}{q_t k_{b,0}^2 a_0^2}, \quad \beta = \frac{2k_{w,0}k_t \mathrm{e}^{(1-\mu)/\epsilon}}{k_{b,0}^2 a_0}, \quad \delta = \frac{k_{b,0}\,\mathrm{e}^{-1/2\epsilon}}{2k_t},$$

$$\mu = \frac{E_w}{2E_b}, \quad \rho = \frac{r k_s w_0 \mathrm{e}^{1/2\epsilon}}{k_{b,0} a_0}.$$

The parameter α is a measure of the quenching effect of the endothermic reaction (4) relative to the heat released from reaction (3), β measures the consumption of the inhibitor W relative to the consumption of the fuel A, μ is effectively the ratio of the activation energies of the temperature dependent reactions and ρ can be regarded as a dimensionless version of the stoichiometry factor r.

The parameter δ measures the rate of the branching reaction (2) relative to the exothermic termination step (3) and, in the present flame context, will be a small parameter. This enables us to simplify our model slightly by putting the terms in Equation (13) involving δ to zero. Thus our model consists of Equations (10–12) together with the algebraic relation

$$x\left((1-v)\,\exp\left(-\frac{(1-u)}{2\epsilon u}\right) - x - \rho\,w\right) = 0,$$

giving

$$x = \begin{cases} (1-v)\,\exp\left(-\frac{(1-u)}{2\epsilon u}\right) - \rho\,w, & \text{if } x > 0 \\ 0, & \text{if } x \le 0 \end{cases}. \tag{15}$$

Ahead of the flame we have

$$u \to 0,\ v \to 0,\ w \to 0,\ x \to 0 \quad \text{as} \quad y \to \infty. \tag{16}$$

If $\rho = 0$, the model (given by Equations (10–12, 16) with x replaced by (15)) simplifies and it is this reduced version of the model that was discussed in [2]. We were then able to combine Equations (10–12) to eliminate the reaction terms [2]. The resulting equation could be integrated and, with boundary conditions (16) applied, gave necessary conditions for front or pulse waves in the temperature. The existence of these two types of wave was confirmed through numerical simulation and through the high-activation-energy asymptotics. Here we are concerned with the situation when $\rho \neq 0$, *i.e.*, when there is an additional quenching effect from the catalytic removal of X by S. In this case we are unable to combine the equations to eliminate the reaction terms and so we cannot derive simple conditions for the formation of front or pulse waves. The most we can say at this stage is that, at the rear of the wave where the reactions are fully completed, we must have $x = 0$ and that pulse (where $u \to 0$) or front (where $u \to u_s > 0$) waves are not precluded.

As a check on the simplification made in (15) we performed numerical simulations of the full system (10–13) with $\delta \neq 0$ for representative parameter values to compare with results obtained using (15). We found that taking δ less than about 10^{-3} was sufficient to give agreement between the two sets of results, at least to graphical accuracy. Further, no additional problems were encountered in the simulations using (15). This suggests that our reduction of the system using (15) is a reasonable approximation provided δ is small.

3. High-activation-energy asymptotics, $\epsilon \ll 1$

In [2] we identified two different cases depending on the relative sizes of the parameters α and β.

(i) when $\alpha \sim \beta$, flame inhibition occurred at a critical value α_{crit} of α through a saddle-node bifurcation. This behaviour is reminiscent of the way flames are extinguished with heat loss by cooling; see [14, 15] for example;

(ii) when $\alpha \ll \beta$, there is no critical value for α, though the flame speed can be reduced considerably as α is increased (for a given value of β).

We examine these two cases for the present model, starting with the case when $\alpha \ll \beta$. For simplicity of exposition we assume unit Lewis numbers, *i.e.*, we take $L_A = L_W = 1$. We expect our results to hold qualitatively for general Lewis numbers provided they are of $O(1)$.

3.1. $\alpha \ll \beta$

In this case the flame has a two-layer structure. There is a thin reaction zone and a thicker preheat zone. To get a consistent matching between the two regions we have to scale $\alpha,\ \beta,\ \rho$ and the wave speed c by, following [2],

$$\alpha = \epsilon^2 \overline{\alpha}, \quad \beta = \epsilon \overline{\beta}, \quad \rho = \epsilon^2 \overline{\rho}, \quad c = \epsilon^{3/2} \overline{c} \tag{17}$$

where $\overline{\alpha},\ \overline{\beta},\ \overline{\rho},\ \overline{c}$ are of $O(1)$ for ϵ small. We start in the preheat zone (region I).

3.1.1. *Preheat zone (Region I)*

Here the reaction terms are negligible (exponentially small). Thus, from (15), $x \equiv 0$. We scale y by

$$\overline{y} = y\,\epsilon^{3/2} \tag{18}$$

and leave $u,\ v,\ w$ unscaled. We apply (17,18) in Equations (10–12) and look for a solution by expanding in powers of ϵ with

$$\overline{c} = c_0 + \epsilon\, c_1 + \cdots . \tag{19}$$

The details are straightforward and we obtain the solution ahead of the flame:

$$\begin{aligned} &u = \mathrm{e}^{-c_0\overline{y}} + \epsilon\left((T_1 - c_1\,\overline{y})\,\mathrm{e}^{-c_0\overline{y}}\right) + \cdots,\ v = \mathrm{e}^{-c_0\overline{y}} + \epsilon(-c_1\,\overline{y}\,\mathrm{e}^{-c_0\overline{y}}) + \cdots, \\ &w = \mathrm{e}^{-c_0\overline{y}} + \epsilon\left((S_1 - c_1\,\overline{y})\,\mathrm{e}^{-c_0\overline{y}}\right) + \cdots, \end{aligned} \tag{20}$$

where T_1 and S_1 are constants to be determined; see [2] for further details. The solutions have been chosen to satisfy boundary conditions (16) and for the leading-order terms to be of $O(1)$ for $\overline{y}$ small. This anticipates the matching with the reaction zone, which is what we now consider.

3.1.2. *Reaction zone (Region II)*
Here we put

$$u = 1 - \epsilon U, \quad v = 1 - \epsilon V, \quad w = 1 - \epsilon W, \quad x = \epsilon X, \quad \zeta = y\,\epsilon^{1/2} = \overline{y}/\epsilon, \tag{21}$$

so that this region is thin, of thickness $O(\epsilon)$ compared to the preheat zone. We apply (21) in Equations (10–12, 15) and look for a solution by expanding

$$U = U_0 + \epsilon\, U_1 + \cdots,\ V = V_0 + \epsilon\, V_1 + \cdots,\ W = W_0 + \epsilon\, W_1 + \cdots,\ X = X_0 + \epsilon\, X_1 + \cdots . \tag{22}$$

Then $X_0 = V_0\,\mathrm{e}^{-U_0/2}$ and the equations for U_0 and V_0 become

$$U_0'' - V_0^2\,\mathrm{e}^{-U_0} = 0, \qquad V_0'' - V_0^2\,\mathrm{e}^{-U_0} = 0, \tag{23}$$

subject to matching with region I, namely

$$U_0 \sim c_0\zeta - T_1 + \cdots, \quad V_0 \sim c_0\zeta \quad \text{as } \zeta \to \infty. \tag{24}$$

Eliminating the reaction terms from Equations (23), integrating and applying the matching conditions (24), we have

$$U_0 = V_0 - T_1. \tag{25}$$

Then substituting (25) in (23) we have, on integrating and applying (24),

$$U_0'^2 = c_0^2 - 2\left((U_0 + T_1)^2 + 2(U_0 + T_1) + 2\right)\,\mathrm{e}^{-U_0}. \tag{26}$$

As $\zeta \to -\infty$, $V_0 \to 0$ (all the fuel is used up in the reaction zone). Hence $U_0 \to -T_1$ and equation (26) gives

$$c_0^2 = 4\,\mathrm{e}^{T_1}. \tag{27}$$

The equation for W_0 is

$$W_0'' - \overline{\beta}\,W_0\,\mathrm{e}^{-\mu U_0} = 0, \qquad W_0 \sim c_0\zeta - S_1 \text{ as } \zeta \to \infty. \tag{28}$$

This is a linear equation for W_0 with U_0 effectively given by (26). The solution must have $W_0 \to 0$ as $\zeta \to -\infty$ (with $W_0 \sim \exp(\sqrt{\overline{\beta}\mathrm{e}^{\mu T_1}}\zeta)$ for $|\zeta|$ large).

At $O(\epsilon)$ we obtain

$$X_1 = \left(V_1 - \frac{V_0(U_0^2 + U_1)}{2}\right) \mathrm{e}^{-U_0/2} - \overline{\rho} \tag{29}$$

and then

$$U_1'' + c_0 U_0' - \mathrm{e}^{-U_0}\left(2V_0V_1 - V_0^2(U_0^2 + U_1)\right) + 2\overline{\rho}V_0\mathrm{e}^{-U_0/2} + \overline{\alpha}W_0\mathrm{e}^{-\mu U_0} = 0, \tag{30}$$

$$V_1'' + c_0 V_0' - \mathrm{e}^{-U_0}\left(2V_0V_1 - V_0^2(U_0^2 + U_1)\right) + \overline{\rho}V_0\mathrm{e}^{-U_0/2} = 0, \tag{31}$$

subject to matching with region I which requires

$$U_1 \sim -\frac{c_0^2}{2}\zeta^2 + (c_0T_1 + c_1)\zeta + T_2 + \cdots, \quad V_1 \sim -\frac{c_0^2}{2}\zeta^2 + c_1\zeta + \cdots, \tag{32}$$

as $\zeta \to \infty$.

Eliminating the terms in e^{-U_0} from Equations (30, 31) and using Equation (28) for W_0, we arrive at an equation that can be integrated once to give, on applying conditions (24, 32),

$$U_1' + c_0U_0 - (V_1' + c_0V_0) + \frac{\overline{\alpha}}{\overline{\beta}}W_0' - \overline{\rho}\int_\zeta^\infty (U_0 + T_1)\mathrm{e}^{-U_0/2}\,\mathrm{d}\zeta = \frac{\overline{\alpha}c_0}{\overline{\beta}}. \tag{33}$$

As $\zeta \to -\infty$, $U_1' \to 0$ so that Equation (33) gives

$$T_1 = -\frac{\overline{\rho}}{c_0}\int_{-\infty}^\infty (U_0 + T_1)\mathrm{e}^{-U_0/2}\,\mathrm{d}\zeta - \frac{\overline{\alpha}}{\overline{\beta}}. \tag{34}$$

We can use expressions (26, 27) in the integral to get

$$I_1 \equiv \int_{-\infty}^\infty (U_0 + T_1)\mathrm{e}^{-U_0/2}\,\mathrm{d}\zeta = \int_0^\infty \frac{s\mathrm{e}^{-s/2}\,\mathrm{d}s}{\sqrt{4 - 2(s^2 + 2s + 2)\mathrm{e}^{-s}}} = 4{\cdot}9283 \tag{35}$$

on evaluating the integral numerically.

Equation (34) reduces to the equation found previously for $\overline{\rho} = 0$, [2]. Applying (34) in Equation (27) we obtain

$$c_0^2 = 4\,\exp\left(-\frac{\overline{\alpha}}{\overline{\beta}} - \frac{\overline{\rho}I_1}{c_0}\right). \tag{36}$$

We can re-write this to give $\overline{\alpha}/\overline{\beta}$ in terms of c_0 as

$$\frac{\overline{\alpha}}{\overline{\beta}} = 2(\log 2 - \log c_0) - \frac{\overline{\rho}I_1}{c_0}. \tag{37}$$

Equation (37) shows that $\overline{\alpha}/\overline{\beta}$ is negative for sufficiently small or large values of c_0 and has a local turning point (maximum) where

$$c_0 = \frac{\overline{\rho}I_1}{2}, \qquad \frac{\overline{\alpha}}{\overline{\beta}} = \left(\frac{\overline{\alpha}}{\overline{\beta}}\right)_{\text{crit}} = 2(2\log 2 - 1 - \log(\overline{\rho}I_1)). \tag{38}$$

Equation (38) shows that, to have $\left(\overline{\alpha}/\overline{\beta}\right)_{\text{crit}} \geq 0$, we must have $\overline{\rho} \leq 4\mathrm{e}^{-1}/I_1 = 0{\cdot}2986$. A typical graph of c_0 against $\overline{\alpha}/\overline{\beta}$ for $\overline{\rho} > 0$ is sketched in Figure 1a. Note that these curves lie below the curve corresponding to $\overline{\rho} = 0$ (shown by the broken line).

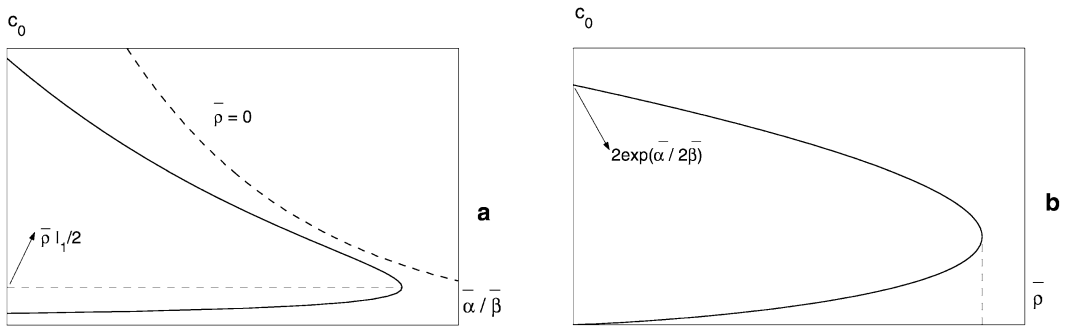

Figure 1. Plots of the wave speed c_0 against (a) $\overline{\alpha}/\overline{\beta}$ (the case for $\overline{\rho} = 0$ is shown by the broken line) and (b) $\overline{\rho}$, obtained from Equation (36).

Figure 1a shows that the effect of the radical scavenger S is to make a qualitative change in the relationship between c_0 and $\overline{\alpha}/\overline{\beta}$. Without this species, $\overline{\rho} = 0$, and there is no inhibition, though the wave speed decreases with increasing values of $\overline{\alpha}/\overline{\beta}$, [2]. Adding this reaction step to the overall process leads to inhibition at a finite value of $\overline{\alpha}/\overline{\beta}$ (through a saddle-node bifurcation) and, if this step is sufficiently strong ($\overline{\rho} > 4\mathrm{e}^{-1}/I_1$), the system is totally quenched. Flames cannot form, even if there is no heat loss from the endothermic decomposition of W, *i.e.*, $\overline{\alpha} = 0$.

An alternative way of viewing Equation (36) is to express $\overline{\rho}$ in terms of c_0 for a given $\overline{\alpha}/\overline{\beta}$, namely

$$\overline{\rho} = \frac{c_0}{I_1}\left(2(\log 2 - \log c_0) - \frac{\overline{\alpha}}{\overline{\beta}}\right). \tag{39}$$

Expression (39) shows that $\overline{\rho} = 0$ at $c_0 = 0$ (with $\overline{\rho} > 0$ for small c_0), $\overline{\rho} = 0$ at $c_0 = 2\,\mathrm{e}^{-\overline{\alpha}/2\overline{\beta}}$ and that $\overline{\rho}$ is large and negative for c_0 large. It has a local turning point (maximum) at

$$c_0 = 2\,\exp(-1 - \frac{\overline{\alpha}}{2\overline{\beta}}), \qquad \overline{\rho} = \overline{\rho}_{\mathrm{crit}} = \frac{4}{I_1}\exp(-1 - \frac{\overline{\alpha}}{2\overline{\beta}}). \tag{40}$$

A graph of c_0 against $\overline{\rho}$ is shown in Figure 1b. This figure shows that we must have $\overline{\rho} < \overline{\rho}_{\mathrm{crit}}$ for flame initiation and emphasises that this additional effect in the kinetic scheme can totally suppress flame propagation.

3.2. $\alpha \sim \beta \ll 1$

We now consider the case when $\alpha \sim \beta \ll 1$. To follow the treatment described in [2] we need α and β to be of $O(\epsilon^4)$ and μ and ρ to be of $O(\epsilon)$. We scale c as in (17) and

$$\alpha = \epsilon^4\tilde{\alpha}, \quad \beta = \epsilon^4\tilde{\beta}, \quad \mu = \epsilon\nu, \quad \rho = \epsilon\tilde{\rho}, \tag{41}$$

where $\tilde{\alpha}$, $\tilde{\beta}$, ν and $\tilde{\rho}$ are all of $O(1)$. In this case we require three regions, regions I and II (preheat and reaction zones) as before, but now there is an additional region III (decay zone) in which the conditions at the rear of the flame are attained.

3.2.1. *Preheat zone (region I)*

We again start in the preheat zone with the scaling for y given by (18) but now we take w to be of $O(\epsilon)$. In this region the exothermic reaction terms are negligible, though there is a (weak)

endothermic reaction since μ is $O(\epsilon)$. Hence, in this region $x \equiv 0$, from (15). The solution is obtained by expanding in powers of ϵ and, following [2] and taking $L_A = L_W = 1$, is

$$\begin{aligned} u &= \mathrm{e}^{-c_0\overline{y}} + \epsilon\left((T_1 - c_1\overline{y})\mathrm{e}^{-c_0\overline{y}} + \frac{\tilde{\alpha}}{\nu c_0}\int_{\overline{y}}^{\infty} \mathrm{e}^{-c_0 s}\exp\left[\nu(1-\mathrm{e}^{c_0 s})\right]\mathrm{d}s\right) + \cdots, \\ v &= \mathrm{e}^{-c_0\overline{y}} + \epsilon\,(-c_1\overline{y}\mathrm{e}^{-c_0\overline{y}}) + \cdots, \\ w &= \epsilon\left(S_1\mathrm{e}^{-c_0\overline{y}} - \frac{\tilde{\beta}}{\nu c_0}\int_{\overline{y}}^{\infty} \mathrm{e}^{-c_0 s}\exp\left[\nu(1-\mathrm{e}^{c_0 s})\right]\mathrm{d}s\right) + \cdots, \end{aligned} \tag{42}$$

where S_1 and T_1 are constants to be found.

3.2.2. *Reaction zone (region II)*

We now turn to the reaction zone, where the scalings are given by (21), though now we put $w = \tilde{W}$. The equations are

$$\begin{aligned} X = V\,\exp\left[-\frac{U}{2(1-\epsilon U)}\right] - \epsilon\tilde{\rho}\tilde{W}, \\ U'' + \epsilon\,\overline{c}\,U' - X^2 + \epsilon^2\tilde{\alpha}(1-\epsilon\tilde{W})\exp\left[-\frac{\epsilon\nu U}{(1-\epsilon U)}\right] = 0, \\ V'' + \epsilon\,\overline{c}\,V' - XV\exp\left[-\frac{U}{2(1-\epsilon U)}\right] = 0, \\ \tilde{W}'' + \epsilon\,\overline{c}\,\tilde{W}' + \epsilon^2\tilde{\beta}(1-\epsilon\tilde{W})\exp\left[-\frac{\epsilon\nu U}{(1-\epsilon U)}\right] = 0, \end{aligned} \tag{43}$$

where primes denote differentiation with respect to ζ. We look for a solution by expanding in powers of ϵ, as in (22). The leading-order problem gives

$$X_0 = V_0\mathrm{e}^{-U_0/2}, \qquad \tilde{W}_0 = S_1 - \frac{\tilde{\beta}J_\nu}{\nu c_0^2} \tag{44}$$

on matching with (42), where

$$J_\nu = c_0\int_0^\infty \mathrm{e}^{-c_0 y}\exp\left[\nu(1-\mathrm{e}^{c_0 y})\right]\mathrm{d}s = \int_0^\infty \frac{\mathrm{e}^{-\nu x}}{(1+x)^2}\,\mathrm{d}x \tag{45}$$

together with Equations (23). Matching with region I now gives

$$U_0 = V_0 - \left(T_1 + \frac{\tilde{\alpha}J_\nu}{\nu c_0^2}\right), \tag{46}$$

where J_ν is defined by (45). Taking $V_0 \to 0$ as $\zeta \to -\infty$ we have

$$U_0 \to -\left(T_1 + \frac{\tilde{\alpha}J_\nu}{\nu c_0^2}\right) \quad \text{as } \zeta \to -\infty. \tag{47}$$

The equation equivalent to (26) is now

$$U_0'^2 = c_0^2 - 2\left((U_0 + T_1 + \frac{\tilde{\alpha}J_\nu}{\nu c_0^2})^2 + 2(U_0 + T_1 + \frac{\tilde{\alpha}J_\nu}{\nu c_0^2}) + 2\right)\mathrm{e}^{-U_0}. \tag{48}$$

Applying condition (47) in (48) now we obtain

$$c_0^2 = 4\,\exp\left(T_1 + \frac{\tilde{\alpha} J_\nu}{\nu c_0^2}\right). \tag{49}$$

At $O(\epsilon)$ we obtain

$$\tilde{W}_1 = -\left(S_1 c_0 - \frac{\tilde{\beta}}{\nu c_0}\right)\zeta \tag{50}$$

from Equation (43d). Equation (43a) gives

$$X_1 = \mathrm{e}^{-U_0/2}\left(V_1 - \frac{V_0}{2}(U_1 + U_0^2)\right) - \tilde{\rho}\tilde{W}_0. \tag{51}$$

We can eliminate the reaction terms from the $O(\epsilon)$ equations derived from (43b,c) (as in Equations (30, 31, 33)) and then, using (44), integrating and matching with (42) we obtain that

$$U_1' = V_1' + \left(c_0 T_1 + \frac{\tilde{\alpha}}{\nu c_0}\right) + \tilde{\rho}\left(S_1 - \frac{\tilde{\beta} J_\nu}{\nu c_0^2}\right)\int_\zeta^\infty \left(U_0 + T_1 + \frac{\tilde{\alpha} J_\nu}{\nu c_0^2}\right)\mathrm{e}^{-U_0/2}\,\mathrm{d}\zeta \tag{52}$$

We now let $\zeta \to -\infty$ in (52). With $V_1' \to 0$, this gives

$$U_1 \sim \left[c_0 T_1 + \frac{\tilde{\alpha}}{\nu c_0} + \tilde{\rho} I_1\left(S_1 - \frac{\tilde{\beta} J_\nu}{\nu c_0^2}\right)\right]\zeta + \cdots \quad \text{as } \zeta \to -\infty, \tag{53}$$

where I_1 is given by (35).

3.2.3. *Decay region (region III)*
The behaviour of u and w, as given by (44, 47, 50, 53), suggests that we need a further region (region III – decay region) in which $v \equiv 1$ (all fuel consumed). Since $v \equiv 1$ in region II, $x \equiv 0$, from (15) and the details for this region are essentially the same as those given in [2]. There are two subregions, region IIIa in which $Y = \epsilon^{3/2} y = \epsilon\,\zeta$ with the corresponding solution

$$u = 1 + \epsilon\left(\frac{\tilde{\alpha}}{c_0} Y + (T_1 + \frac{\tilde{\alpha} J_\nu}{\nu c_0^2})\right) + \cdots, \quad w = \epsilon\left(-\frac{\tilde{\beta}}{c_0} Y + (S_1 - \frac{\tilde{\beta} J_\nu}{\nu c_0^2})\right) + \cdots. \tag{54}$$

Matching with (44, 47, 50, 53) then gives

$$S_1 = \frac{\tilde{\beta}(\nu+1)}{\nu c_0^2}, \quad T_1 = -\left(\frac{\tilde{\alpha}(\nu+1)}{\nu c_0^2} + \frac{\tilde{\rho}\tilde{\beta} I_1(1+\nu - J_\nu)}{\nu c_0^3}\right) \tag{55}$$

The expression for T_1 in (55) is the same as that given in [2] when $\tilde{\rho} = 0$.

In region IIIb we put $\xi = \epsilon^{5/3} y = \epsilon Y$, obtaining the leading-order problem

$$c_0 u' - \tilde{\alpha}(1-w)\exp[-\nu(1-u)/u] = 0, \quad c_0 w' + \tilde{\beta}(1-w)\exp[-\nu(1-u)/u] = 0, \tag{56}$$

where primes now denote differentiation with respect to ξ, subject to

$$u \sim 1 + \frac{\tilde{\alpha}}{c_0}\xi + \cdots, \quad w \sim -\frac{\tilde{\beta}}{c_0}\xi + \cdots, \quad \text{as } \xi \to 0^- \tag{57}$$

on matching with region IIIa. Combining equations (56), integrating and applying (57) we obtain

$$\tilde{\beta}u + \tilde{\alpha}w = \tilde{\beta} \tag{58}$$

and then

$$c_0 u' - (\tilde{\alpha} - \tilde{\beta} + \tilde{\beta}u)\exp[-\nu(1-u)/u] = 0, \tag{59}$$

subject to (57). As in [2], Equation (59) shows that we can have front waves if $\tilde{\alpha} < \tilde{\beta}$, with $u \to 1 - \tilde{\alpha}/\tilde{\beta}$, $w \to 1$ as $\zeta \to -\infty$, or pulse waves if $\tilde{\alpha} > \tilde{\beta}$, with $u \to 0$, $w \to \tilde{\beta}/\tilde{\alpha}$ as $\zeta \to -\infty$.

We now return to the expression for the wave speed c_0 obtained from expressions (49) and (55).

3.2.4. *Wave speed*

Application of (55) in (49) gives

$$c_0^2 = 4\,\exp\left(-(\frac{\nu + 1 - J_\nu}{\nu})(\frac{\tilde{\alpha}}{c_0^2} + \frac{\tilde{\rho}\tilde{\beta}I_1}{c_0^3})\right). \tag{60}$$

We can express Equation (60) as

$$\tilde{\alpha} = \frac{2\nu}{(\nu + 1 - J_\nu)}\,c_0^2(\log 2 - \log c_0) - \frac{\tilde{\rho}\tilde{\beta}I_1}{c_0} \tag{61}$$

Note that $J_\nu < 1$ for $\nu > 0$, hence expression $\frac{2\nu}{\nu+1-J_\nu}$ is positive for all $\nu > 0$. Equation (61) shows that $\tilde{\alpha}$ is large and negative for both small and large values of c_0 and has a turning point where

$$c_0^3(2\log c_0 + 1 - 2\log 2) = \frac{(\nu + 1 - J_\nu)\tilde{\rho}\tilde{\beta}I_1}{2\nu}. \tag{62}$$

The left-hand side of Equation (62) is negative for $c_0 < 2\mathrm{e}^{-1/2}$ and positive and monotone increasing for $c_0 > 2\mathrm{e}^{-1/2}$. Since the right-hand side is positive (for $\nu > 0$), there is only one turning point for Equation (61) for $c_0 > 0$ which must occur at a value of $c_0 > 2\mathrm{e}^{-1/2}$. Thus a necessary condition for $\tilde{\alpha} \geq 0$ at the turning point is that $\tilde{\rho} < \frac{8\nu\mathrm{e}^{-3/2}}{(\nu+1-J_\nu)\tilde{\beta}I_1}$. A sketch of the $c_0 - \tilde{\alpha}$ curve for this case is shown in Figure 2a. Also shown in Figure 2a is the corresponding curve for $\tilde{\rho} = 0$ (by the broken line). The figure shows that the values of c_0 for a given value of $\tilde{\alpha}$ are reduced from those when $\tilde{\rho} = 0$ and that the critical value of $\tilde{\alpha}$ is less when $\tilde{\rho} \neq 0$. Thus the effect of the radical scavenger is to reduce the range over which flames can form and, if the effect is sufficiently strong, to totally quench the system.

Alternatively, we can express Equation (60) in terms of $\tilde{\rho}$ as

$$\tilde{\rho} = \frac{1}{\tilde{\beta}I_1}\left(\frac{2\nu}{\nu + 1 - J_\nu}\,c_0^3(\log 2 - \log c_0) - \tilde{\alpha}c_0\right). \tag{63}$$

Equation (63) has $\tilde{\rho} = 0$ at $c_0 = 0$ with $\tilde{\rho} < 0$ for small and large c_0, with, when $\tilde{\alpha} > 0$, two zeros on $c_0 > 0$. A graph of $\tilde{\rho}$ against c_0 is sketched in Figure 2b. The graph for the case when $\tilde{\alpha} = 0$ is similar to that shown in Figure 2b, though now the curve crosses the c_0-axis only once and on the lower branch $c_0 \to 0^+$ as $\tilde{\rho} \to 0$. Both these graphs shows that there

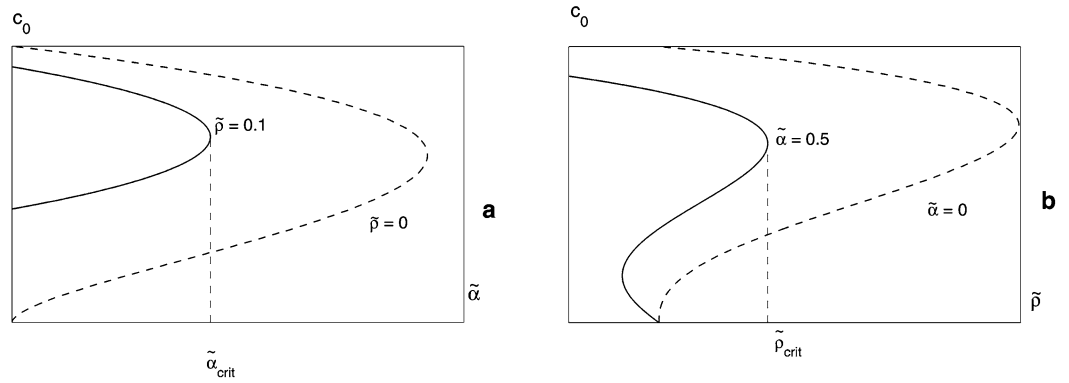

Figure 2. Plots of the wave speed c_0 against (a) $\tilde{\alpha}$ for a given $\tilde{\rho}$, the curve for $\tilde{\rho} = 0$ is shown by the broken line, (b) $\tilde{\rho}$ for a given $\tilde{\alpha}$ for $\tilde{\alpha} > 0$, obtained from Equation (60).

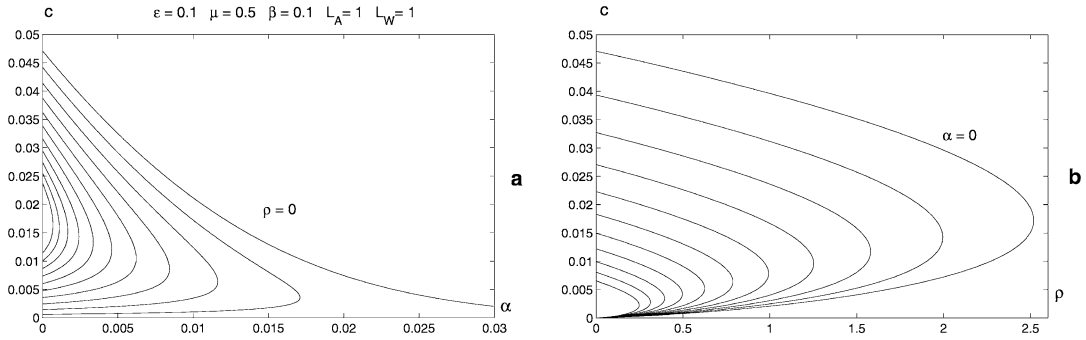

Figure 3. Plots of the wave speed c against (a) α for given values of ρ, (from $\rho = 0$ to $\rho = 0{\cdot}0024$) (b) ρ for given values of α, (from $\alpha = 0$ to $\alpha = 0{\cdot}0211$) with $\epsilon = 0{\cdot}1,\ \beta = 0{\cdot}1$ representative of the high activation energy asymptotics for $\alpha \ll \beta$ (see Section 3.1). $L_A = L_W = 1{\cdot}0$, $\mu = 0{\cdot}5$.

is a critical value for $\tilde{\rho}$ for wave formation and emphasise the quenching effect of the radical scavenger.

4. Numerical solutions

We solved the propagating flame Equations (10–12, 15, 16) numerically with a small value of ϵ, taking $\epsilon = 0{\cdot}1$, for parameter values representative of the two cases treated by high-activation-energy asymptotics. For the first case, $\alpha \ll \beta,\ \beta$ of $O(\epsilon)$, we took $\beta = 0{\cdot}1$ and for the second case, $\alpha \sim \beta \sim \epsilon^4$, we took $\beta = 10^{-4}$. Our results are presented as plots of the wave speed c against α, for fixed values of ρ and plots against ρ for fixed values of α. In both cases we considered only unit Lewis numbers, $L_A = L_W = 1$, in line with the theoretical description and took $\mu = 0.5$.

The results for $\beta = 0{\cdot}1$ are shown in Figure 3. The plots of c against α shown in Figure 3a have the same general features as the sketch in Figure 1a obtained from the high-activation-energy asymptotics. They both show the same qualitative difference between the the cases $\rho = 0$ (no inhibition though a reducing propagation velocity as α increases) and $\rho > 0$, where there is a critical value α_{crit} for α for flame propagation. The figure also shows that there is a bound on ρ to have flames even in the 'adiabatic' ($\alpha = 0$) limit. For the parameters used for Figure 3a this value is $\rho = 0{\cdot}0025$, which compares reasonably well with the value

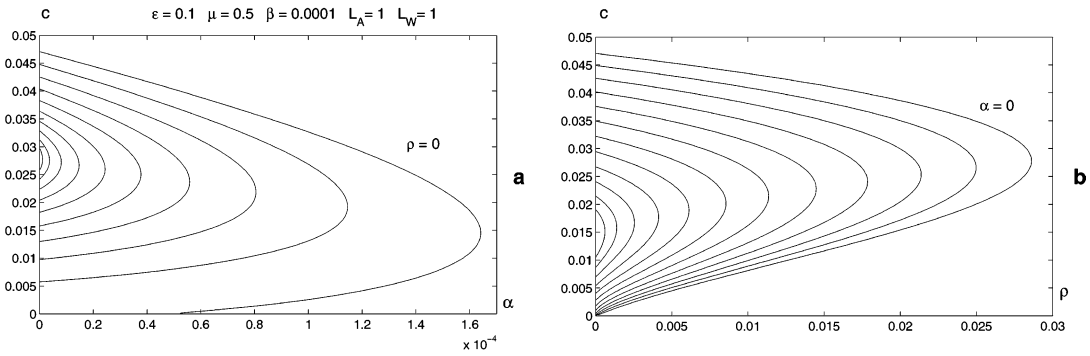

Figure 4. Plots of the wave speed c against (a) α for given values of ρ (from $\rho = 0$ to $\rho = 0{\cdot}0283$), (b) ρ for given values of α, (from $\alpha = 0$ to $\alpha = 1{\cdot}587 \times 10^{-4}$) with $\epsilon = 0{\cdot}1$, $\beta = 10^{-4}$ representative of the high activation energy asymptotics for $\alpha \sim \beta$ (see Section 3.2). $L_A = L_W = 1{\cdot}0$, $\mu = 0{\cdot}5$.

of $\rho = 0{\cdot}0030$ obtained from the high-activation-energy asymptotics. In Figure 3b we give plots of c against ρ for increasing values of α (the case $\alpha = 0$ is labelled). These curves have the same qualitative form as that sketched in Figure 1b and decrease in extent as α is increased to α_{crit}. This figure shows more clearly the existence of a critical value for ρ for flame propagation in the $\alpha = 0$ limit.

Figure 4 gives plots for $\beta = 10^{-4}$. Both figures again have the same qualitative shapes as those sketched in Figures 2a and 2b, the parts of the curve for $\rho < 0$ in Figure 2b are not shown in Figure 4b. Here there is a critical value of α for wave propagation in the $\rho = 0$ limit and this value decreases, with the corresponding wave speeds also decreasing, as ρ is increased. As predicted by the high-activation-energy asymptotics there is total flame quenching for a sufficiently large value of ρ. This value was found to be $\rho = 0{\cdot}0286$ for the parameters used for Figure 4a. This compares reasonably well with the value of $\rho = 0{\cdot}024$ obtained from the high-activation-energy asymptotics. Figure 4b again shows flame inhibition for a critical value of ρ, even in the $\alpha = 0$ limit.

5. Conclusions

The main conclusion from our study is that the radical scavenger can have a strong additional inhibitory effect on flame propagation. There are two processes in our model that have a decelerating effect on the exothermic combustion reactions, namely the endothermic decomposition of an inhibitory species W and the removal of the active radical X by a scavenger species S. Both processes reduce the flame propagation speed, sometimes quite considerably, and can inhibit flame propagation altogether.

We identified two distinct cases, namely relatively fast and relatively slow decomposition of W, through the parameter β changing by a few orders of magnitude. In the first case, the decomposition of W alone does not inhibit flame propagation, its effect is only to slow down the propagation speed as the 'heat loss' parameter α is increased. The effect of the radical scavenger is to make a qualitative change in this behaviour, now there is a critical value α_{crit} of α for possible flame propagation. In the latter case there is a critical α_{crit} even with no radical scavenger ($\rho = 0$) for flame propagation. The effect of the radical scavenger does not change this but does decrease the value of α_{crit}. In both cases flame propagation can be

totally suppressed by a sufficiently large production of S from the decomposition of W through reaction (4).

Our high-activation-energy asymptotics allows us to assess the effect of the radical scavenger S on the flame. The active radical X is produced within the reaction zone by the branching step (2) and its recombination via step (3) produces the heat necessary to sustain the flame. The main effect of the inhibitor W is to reduce the temperature within the reaction zone (in the asymptotic solution to decrease the constant T_1 from its adiabatic value of zero). If the consumption of W within the preheat zone is sufficiently large (higher values of β), then the relatively small amount of W left to react within the reaction zone is unable on its own to remove sufficient heat to inhibit the flame. If less W is consumed within the preheat zone (smaller values of β), this is not the case and there can be enough W left in the reaction zone to allow decomposition reaction (4) to remove sufficient heat for flame extinction.

This method of flame extinction, the thermal effect, is an interaction between the heat loss in the reaction zone and the consumption of the inhibitor W in the preheat zone and thus occurs over the full extent of the flame. The effect of the radical scavenger, the chemical effect, is more local and is seen only within the reaction zone. Its main effect on flame extinction is to reduce the the temperature within the reaction zone (see Equations (34) and (35)) by reducing the concentration of X within the reaction zone. Thus the effect of the radical scavenger is more critical on flame inhibition than the endothermic heat loss as it acts on the central core of the flame. Small reductions in the concentration of X in the reaction zone can lead to considerable reductions in temperature with the consequently very much reduced rates for the exothermic combustion reactions.

These effects were brought out from our high-activation-asymptotic energy analysis, and confirmed by numerical integrations for some representative cases. This shows clearly the usefulness of this approach. Here we extended results derived previously [2] to include the effects of the radical scavenger. For the small β case (Section 3.2) we took μ, the ratio of the activation energies, to be small so as to follow the results given in [2]. In a subsequent study with a first-order combustion reaction [3] we have been able to remove this restriction. With μ of $O(1)$ the regions where the combustion and decomposition reactions take place separate out within the flame in the small ϵ limit. A consideration of the 'small β' case for this reaction with μ of $O(1)$ has shown the existence of further solution branches, with up to three flame solutions for a given value of β. This high-activation-energy analysis is applicable to the second-order reaction model considered here and in [2], with the obvious extension to include the radical scavenger.

Previous studies, using a different theoretical approach to model the chemical effect [18, 19], report bifurcation diagrams that are qualitatively similar to those derived here and given in [3, 16]. This work also shows that the chemical effect can have a strong influence on flame propagation (reducing the flame speed), lead to (further) multiple solution branches and induce flame inhibition. Experimental observations by Mitani [20] show considerable reductions in flame speeds and flame quenching when powders, $NaHCO_3$, and gaseous retardants, CF_3Br, are added to the fuel. Further experimental evidence is provided by counter-flow flames [7, 9] which show that pure-water mist reduces the extinction limit for stable flames and that, by adding NaCl to the water mist, reduces this extinction limit even further.

Our results have been confined to unit Lewis numbers. The effect of having different Lewis numbers has been considered for the first-order reaction model [16], where it was seen that the nature of the flame solutions was not qualitatively changed. However, having non-unit Lewis numbers did change the stability of the flames, with Hopf bifurcations occurring leading to

oscillatory propagation. Similar behaviour is seen in the second-order combustion reaction model, both in the existence of flame solutions and in their stability, though the additional effect of the radical scavenger could make significant differences to the stability of these flames. This is, at present, under consideration [17] and will be reported on later.

Acknowledgements

The authors wish to acknowledge the help received from the ESF Programme REACTOR and AL wishes to thank ORS and the University of Leeds for financial support.

References

1. B.F. Gray, S. Kalliadasis, A. Lazarovici, C. Macaskill, J.H. Merkin and S.K. Scott, The suppression of an exothermic branched-chain flame through endothermic reaction and radical scavenging. *Proc. R. Soc. London* A458 (2002) 2119–2138.
2. A. Lazarovici, S. Kalliadasis, J.H. Merkin and S.K. Scott, Flame quenching through endothermic reaction. *J. Engng. Math.* 44 (2002) 207–228.
3. P. Simon, S. Kalliadasis, J.H. Merkin and S.K. Scott, Inhibition of flame propagation by an endothermic reaction. *IMA J. Appl. Math.* 68 (2003) 1–26.
4. P. Simon, S. Kalliadasis, J.H. Merkin and S.K. Scott, Quenching of flame propagation through endothermic reaction. *J. Math. Chemistry* 32 (2002) 73–98.
5. T. Mitani and T. Niioka, Comparison of experiments and theory on heterogeneous flame suppressants. In: *19th Symposium Combustion* Combustion Institute, Pittsburg, PA (1982) pp. 869–875.
6. T. Mitani and T. Niioka, Extinction phenomenon of premixed flames with alkali metal compounds. *Combust. Flame* 55 (1984) 13–21.
7. R. Zheng, K.N.C. Bray and B. Rogg, Effects of sprays of water and NaCl-water solution on the extinction of laminar premixed methane-air counter-flow flames. *Combust. Sci. Technol.* 126 (1997) 389–401.
8. A.M. Lentati and H.K. Chelliah, Dynamics of water droplets in a counterflow field and their effect on flame extinction. *Combust. Flame* 115 (1998) 158–179.
9. B. Mesli and I. Gokalp, Extinction limits of opposed jet turbulent premixed methane air flames with sprays of water and NaCl-water solution. *Combust. Sci. Technol.* 153 (2000) 193–211.
10. G. Joulin, A. Liñan, G.S.S. Ludford, N. Peters and C. Schmidt-Laine, Flames with chain-branching/chain-breaking kinetics. *SIAM J. Appl. Math.* 45 (1985) 420–434.
11. M.A. Birkan and C.K. Law, Asymptotic structure and extinction of diffusion flame with chain mechanism. *Combust. Flame* 73 (1988) 127–146.
12. B.H. Chao and C.K. Law, Laminar flame propagation with volumetric heat loss and chain branching-termination reactions. *Int. J. Heat Mass Transfer* 37 (1994) 673–680.
13. M. Marion, Qualitative properties of a nonlinear system for laminar flames without ignition temperature. *Nonlinear Anal.* 9 (1985) 1269–1292.
14. J. Buckmaster, The quenching of deflagration waves. *Combust. Flame* 26 (1976) 151–162.
15. P. Simon, S. Kalliadasis, J.H. Merkin and S.K. Scott, Quenching of flame propagation with heat loss. *J. Math. Chemistry* 31 (2002) 313–332.
16. P. Simon, S. Kalliadasis, J.H. Merkin and S.K. Scott, Stability of flames in an exothermic-endothermic system. Accepted for publication in *IMA J. Appl. Math.*
17. P. Simon, S. Kalliadasis, J.H. Merkin and S.K. Scott, The effect of a radical scavenger on the propagation of flames in an exothermic-endothermic system. (In preparation).
18. T. Mitani, A flame inhibition theory by inert dust and spray. *Combust. Flame* 43 (1981) 243–253.
19. T. Mitani, A study on thermal and chemical effects of heterogeneous flame suppressants. *Combust. Flame* 44 (1982) 247–260.
20. T. Mitani, Flame retardants effects of CF_3Br and $NaHCO_3$. *Combust. Flame* 50 (1983) 177–188.